MADYMO Modeling of the IHRA Head-form Impactor

Sarath-Babu Kamalakkannan and Dennis A. Guenther
The Ohio State University
Columbus, OH

John F. Wiechel
SEA Limited, Inc.
Worthington, OH

Jason Stammen
US DOT/NHTSA Vehicle Research & Test Center
East Liberty, OH

ABSTRACT

The International Harmonization Research Activities Pedestrian Safety Working Group (IHRA PSWG) has proposed design requirements for two head-forms for vehicle hood (bonnet) impact testing. This paper discusses the development of MADYMO models representing the IHRA adult and child head-forms, validation of the models against laboratory drop tests, and assessment of the effect of IHRA geometric and mass constraints on the model response by conducting a parameter sensitivity analysis. The models consist of a multibody rigid sphere covered with a finite element modeled vinyl skin.

The most important part in developing the MADYMO head-form models was to experimentally determine the material properties of the energy-absorbing portion of the head-form (vinyl skin) and incorporate these properties into MADYMO using a suitable material model. Three material models (linear isotropic, viscoelastic, hyperelastic) were examined. It was determined that the vinyl material behaved as a hyperelastic material when comparing MADYMO simulation results with laboratory certification test results. The MADYMO model of the IHRA adult head-form was validated with laboratory head-form drop tests from four different heights. Parameter sensitivity analysis was conducted by varying the head-form parameters within their respective IHRA tolerances. Because of physical limitations of locating accelerometers near the head-form center of gravity, this analysis was much more easily accomplished using a MADYMO model. It was found that the peak acceleration was well within the IHRA–specified range for both the adult and child head-forms when the mass and geometric parameters were varied within the IHRA tolerances.

INTRODUCTION

Pedestrians killed by motor vehicles represent one of the largest health hazards in the world. Since 1991, approximately 5,000 pedestrians have been killed in traffic crashes every year in the United States (Figure 1). In developing countries such as Ethiopia and Zambia, pedestrian deaths outnumber occupant deaths [19]. In an automobile-pedestrian collision, commonly injured body regions of pedestrians include the lower extremities (pelvis and legs), head, and chest [3, 6, 7]. Common vehicle sources for those injuries are the front bumper, hood (bonnet), windshield (windscreen), and windshield (windscreen) frame/A-pillars [3, 7]. Several studies [3, 6, 7, 12] have shown that head injury is the most fatal and most severe of all pedestrian injuries (Figure 2). The leading sources of head injury to pedestrians in passenger cars are the hood (bonnet), windshield (windscreen) and A-pillars [7].

Minimizing vehicle aggressiveness towards pedestrians is one way to approach pedestrian protection. The International Harmonization Research Activities Pedestrian Safety Working Group (IHRA PSWG) is aimed at establishing harmonized test procedures that would reflect the accident conditions in IHRA member countries. These procedures would prompt the improvement of vehicle structures for the reduction of fatalities and alleviation of severe injuries in pedestrian vs. passenger car crashes [7]. IHRA PSWG has specified requirements for two head-form designs for vehicle hood (bonnet) impact testing (Figure 3).

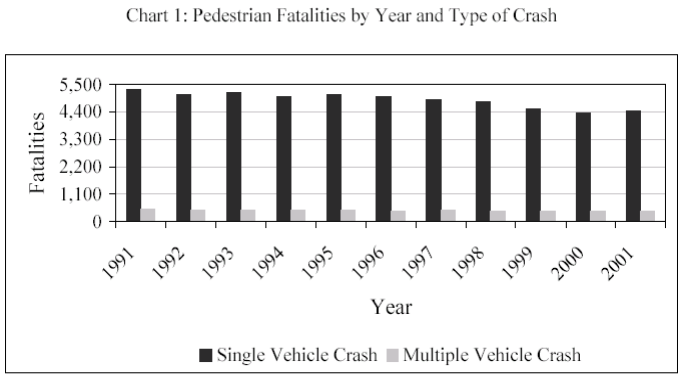

Figure 1 Pedestrian fatalities by year and type of crash

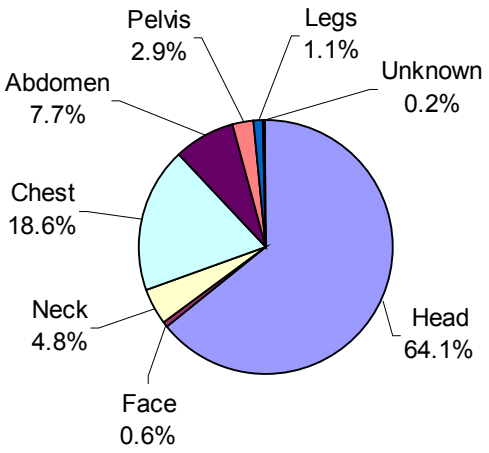

Figure 2 Distribution of AIS 4-6 injuries in IHRA database [7]

Table 1 IHRA head-form characteristics

Requirement description	Child head-form	Adult head-form
Mass (kg)	3.5 +/- 0.1	4.5 +/- 0.1
Diameter (mm)	165 +/- 1	165 +/- 1
Distance from head CG to center of sphere (mm)	<10	<10
Seismic mass distance from center of sphere (mm)	<10	<10
Head drop acceleration (g)	245 - 300	225 – 275

Figure 3 IHRA child (left) and adult (right) head-form devices

The head-forms consist of a solid aluminum core, a vinyl skin, an accelerometer mount, and an accelerometer mounted within a radius of 10mm from the spherical center of the head-form. The IHRA head-forms have specified parameters such as mass, diameter, center of gravity location and accelerometer position. The values for these parameters and their respective tolerances are given in Table 1. Varying these parameters within their respective tolerances might cause a considerable variation in the acceleration time histories measured during testing. Studying the effect of varying these parameters using a mathematical model would be more cost effective and less time consuming than physically adjusting them within the head-form.

Various methods and techniques have been used over the years to study head injuries using mathematical head models. Ruan et al. [13] developed a 3-D human head finite element model and validated it against cadaveric test data in frontal impact. The validated model was used to conduct a parametric study of intracranial pressure, maximum shear stress in the brain, and von Mises stress in the skull. Willinger et al. [17] developed a 3D finite element human head model with a realistic geometry integrating a skull fracture simulation capability. The skull mesh was obtained by digitalizing the external and internal surface of a human skull and skull properties were based on established bone mechanical properties. The model was validated and could be a powerful tool to predict the aggressiveness level of a head impact. Takhounts et al. [15] developed a mathematical surrogate of the human head (SIMon) that is able to solve approximately 30,000 equations every millisecond. This model was designed to best replicate all available experimental data and is not meant to simulate the proper response of every region of the head. Kleiven et al. [9] developed a parameterized finite element (FE) model of the human head and validated it against cadaver experiment data. In the parameterized model, the geometry could be adjusted to fit a particular specimen, which would reduce some of the concerns associated with scaling. Zhang et al. [18] developed a new version of the 3-D finite element model of the Wayne State Brain Injury Model (WSUBIM). This model featured detailed anatomical characteristics of the human head including an

anatomically realistic facial model and was validated against published cadaver test data.

Although a lot of work had been done on modeling the human head, limited research has been done on head-form modeling. A comparison of some of the available mathematical head-form models is given in Table 2. Nakahama et al [11] studied the application of finite element simulations to the impact phenomena of a rigid head-form against deformable plastic plates. An explicit FE code was used for the simulation. The material properties of the plastic plates were obtained by conducting static and dynamic material tests using a static loading machine and split hopkinson pressure bar method respectively. The head-form impact against the plastic plates was validated with data from three different impact speeds of 2.2, 4.4 and 6.7 m/s. Sugita et al. [14] developed a featureless head-form using PAM-CRASH. The dummy skin was modeled using a crushable foam material law and the material properties were derived from static compression test data. The model was validated with data from a standard head drop test at 2.68 m/s. Bilkhu et al. [2] developed a rubber like head-form skin model using LSDYNA3D. The skin was modeled using an elastic-plastic hydrodynamic material law based on data derived from a uni-axial quasi-static test. The model was validated with data obtained from a 6.71 m/s head drop test. Barbat et al. [1 & 3] modeled the dummy skin using linear viscoelastic material in PAM-CRASH and RADIOSS. The material properties for the dummy skin were derived from high velocity head drop tests. The model was validated with data from drop tests at 2.68, 4.02 and 6.71 m/s. Chou et al. [3] developed a deformable featureless head-form model using LSDYNA3D and FCRASH. The head skin was modeled using viscoelastic material. Parameters for the viscoelastic material were determined by comparing the predicted head-form responses with data from head drop tests at different velocities of 2.68, 4.02 and 6.71 m/s. The effect of number of layers (1 to 4) of solid elements across the thickness of the skin was studied using this material model.

Table 2 Comparison of various mathematical head-form models

Developed by	FE Software/approach used	Material type	Experiment/method used to determine material properties	Head-form model validation	Reference
Nakahama et al. 1992	An explicit FE code	Rigid body	Not Applicable	Impact against plastic plates @ 2.2, 4.4 and 6.7 m/s	[11]
Sugita et al. 1995	PAM-CRASH	Crushable foam	Static compression testing of dummy skin	Standard head drop test @ 2.68 m/s	[14]
Bilkhu et al. 1995	LS-DYNA3D	Elastic-plastic hydrodynamic	Uni-axial quasi-static test	Head drop test @ 2.68 and 6.71 m/s	[2]
Barbat et al. 1996	PAM-CRASH & RADIOSS	Viscoelastic	High velocity head drop tests	Head drop test @ 2.68, 4.02 and 6.71 m/s	[1 & 3]
Chou et al. 1997	LS-DYNA3D & FCRASH	Viscoelastic	Trial & error and optimization technique through design of experiment method	Head drop test @ 2.68, 4.02 and 6.71 m/s	[3]
Konosu et al. 2000	MADYMO	Not known	Not known	Head drop certification test and head-form to bonnet top test	[10]
Deb et al. 2004	LSDYNA/Lumped parameter based approach	Elasto-plastic	Assumed values for spring stiffness	Head drop @ 6.7 m/s and head-form impact tests in the upper interior of vehicle	[5]

Konosu, et al., [10] developed a computer simulation MADYMO model of the European Enhanced Vehicle-Safety Commission (EEVC) pedestrian subsystem impactors, which included the adult and child head-forms. The model was intended to promote the development of pedestrian friendly cars by simulating head-form drop tests on cars. Though the models showed good agreement with the values obtained from subsystem tests, some improvements would be needed to apply it to simulate subsystem tests on cars. Deb, et al., [5] developed a nonlinear lumped mass model for simulating head-form impact with rotation on a stiff target with countermeasures for HIC reduction. Results from the model were verified against an equivalent finite element based model using LS-DYNA. The model could be used as a good tool for head impact safety evaluation in the preliminary design phase of vehicles. The model also gave an indication of about how head-form rotation could reduce HIC.

The International Harmonization Research Activities (IHRA) proposed two head-forms to be used internationally to evaluate vehicle-head impact response [7]. The IHRA head-form's parameters such as mass, diameter, center of gravity location and accelerometer location, have tolerances within which these parameters can be varied. Within these tolerances the head-form is supposed to have response characteristics in a prescribed range (i.e. peak acceleration should be within 225 – 275 g for the adult head-form in a certification test). No tests have been performed on the IHRA head-form to confirm this design objective. It is highly impractical to vary these parameters within the respective tolerances and hence a computer model of the head-form would better study the effect of these parameters on the response characteristics of the head-form. A computer simulated model would facilitate evaluating the head-form itself as well as the effect of placement of instrumentation. Development of such a model requires sufficient detail to replicate appropriate response and at the same time requires adequate generalization to allow for greater utility. No computer simulation model of the IHRA head-form currently exists.

The most important aspect of modeling the head-form is assigning the appropriate material model to the head-form skin and determining the appropriate material properties for this material model. Previous researchers have used crushable foam, elasto-plastic and viscoelastic material models for the head-form skin. The only MADYMO model of a head-form is for the EEVC head-form and was developed by Konosu, et al., [10]. However, Konosu did not publish the material properties that he used for the head-form skin.

The objectives of the research discussed in this paper are to

1. Develop MADYMO models simulating the response characteristics of the IHRA pedestrian head-form impacts
2. Validate the MADYMO head-form models using laboratory drop tests
3. Conduct a parameter sensitivity analysis; i.e., study the change in head-form acceleration and HIC by varying the head-form parameters within their respective limits of tolerances.

MATERIALS AND METHODS

MADYMO (MAthematical DYnamic MOdel) is a computer program that simulates the dynamic behavior of physical systems, emphasizing the analysis of vehicle collisions, the biomechanical response of persons involved in vehicle collisions, and assessing the sustained injuries [30]. MADYMO is a multibody system model and includes an explicit FE code that uses a Lagrangian description. The IHRA head-form model was developed using MADYMO. The model of the IHRA head-form is characterized by its geometry as well as its inertial and material properties. The mass, center of gravity, and the mass moments of inertia of the head-form were obtained from the manufacturer. The aluminum core and the accelerometer mount are rigid and they mainly contribute to the inertial properties whereas the vinyl skin undergoes elastic deformation during impact. In MADYMO, the aluminum core and accelerometer mount are represented by a multibody sphere to make the model simple. The vinyl skin is modeled using finite elements. The geometry and finite element mesh for the vinyl skin are implemented using ABAQUS and imported into MADYMO. The vinyl skin is modeled as a hollow hemisphere with eight node hexahedral (brick) elements. Figure 4 shows the FE vinyl skin, which consists of 600 elements and 963 nodes. The average length for each element is assigned to be 12 mm.

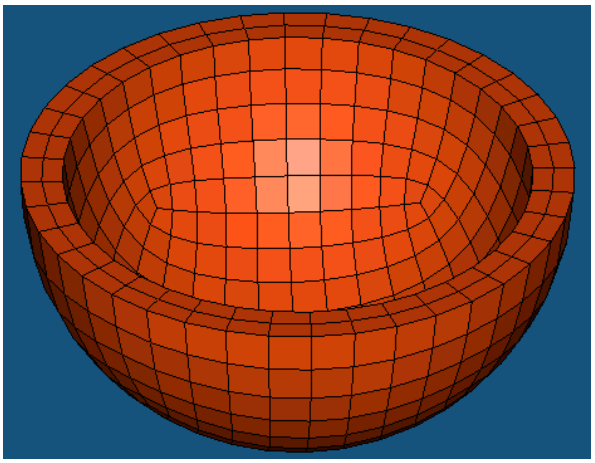

Figure 4 Finite element vinyl skin of the IHRA head-form

SIMULATION OF THE CERTIFICATION TEST

Figure 5 shows the test set up for the head-form impactor certification test. When the head-forms are dropped in a certification test, the peak acceleration values should be within the range specified in Table 1 [7]. The steel plate used in the certification test is

modeled as a rigid plane using four node quadrilateral elements. The finite element plane consists of 289 elements and 324 nodes. Although the drop height in the physical test is 376 mm, the drop height in the simulation was selected as 5 mm. The initial velocity of the head-form in the simulation was then adjusted to compensate for this reduced drop height such that the velocity of the model at impact is same as in the laboratory test. This is done to reduce the large number of data points due to high sampling rate and also to reduce the simulation time. The gravity field, which is a field based contact, is applied to the head-form. The contact between the head-form model and the plate is defined using a penalty-based contact. The two singular criteria often used to evaluate head injury are peak acceleration and HIC. These parameters are more easily compared when evaluating the model and are used in this study to quantify the ability of the model to mimic the head-form impactor. Head Injury Criteria (HIC) has been shown to be an effective indicator of head injury and has been used almost universally in crash injury research and prevention. HIC is given by,

$$\text{HIC} = \max_{t_1, t_2 \rightarrow} \left\{ (t_2 - t_1) \left[\frac{1}{(t_2 - t_1)} \int_{t_1}^{t_2} a(t)dt \right]^{2.5} \right\} \quad (1)$$

Where a(t) is the resultant acceleration history, t_1 and t_2 are two points in time which would maximize the HIC value, and (t_2 - t_1) is the maximum time interval. The HIC algorithm in MADYMO is based on the algorithm developed by Mentzer [16]. In MADYMO, the maximum time interval for HIC is selected to be 36 ms

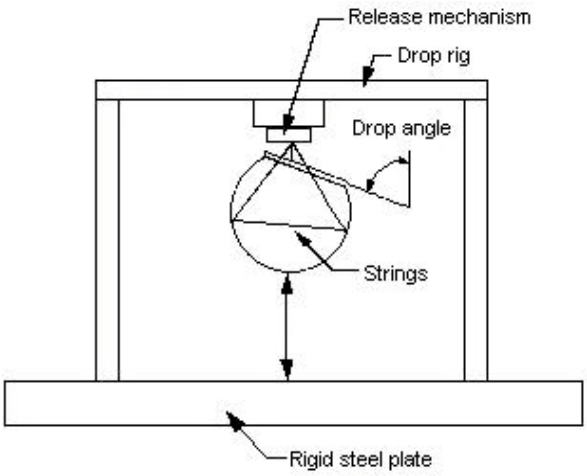

Figure 5 Test set up for head-form impactor certification test

MATERIAL MODEL

Of all the material models available in MADYMO, three are relevant to vinyl materials. They are isotropic elastic, viscoelastic and hyperelastic material models. The material parameters for the three material models were determined experimentally. A detailed description on arriving at the hyperelastic material parameters is found in [8]. Experimental data was fitted with the following equation to obtain the hyperelastic material parameters,

$$\sigma_1 = 2A\lambda_1^2 - \frac{2A}{\lambda_1} + 2B\lambda_1 - \frac{2A}{\lambda_1^2} \quad (2)$$

Where σ_1 is the 2nd Piola-Kirchoff stress, λ_1 is the stretch scalar and A and B are hyperelastic material parameters.

The values for hyperelastic material parameters A and B obtained for the vinyl material were A = -1.1e6 N/m^2 and B = 1.1e6 N/m^2. A limitation of MADYMO is that neither A nor B can be negative and hence the derived values for A and B could not be used in MADYMO. This restriction prevents the accurate representation of certain materials such as the vinyl from being modeled here. Although this limitation will be lifted in the future versions of MADYMO, such limitations remained for this study. Given the restriction of only positive values for A and B, the asymptotic values of A and B derived above were adjusted to be positive values to give a reasonable fit to equation (2). Figure 6 shows the comparison between the derived A and B and adjusted positive A and B values plotted using equation (2). The adjusted positive values for the hyperelastic parameters were A = 6e4 N/m^2 and B = 5e5 N/m^2.

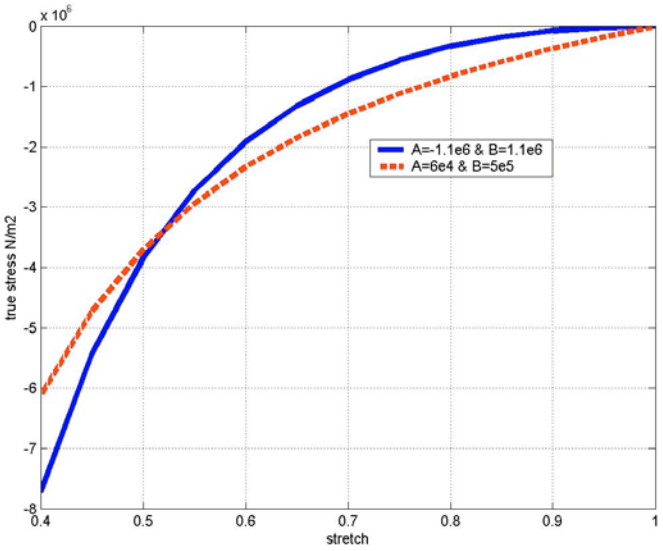

Figure 6 Positive hyperelastic parameters A and B for the vinyl skin in MADYMO model of the IHRA head-form

These material parameters were used in the MADYMO simulations. By comparing the experimental and simulated results of the certification test, it was found that the isotropic elastic and viscoelastic material models are not appropriate to model the vinyl material of the head-form skin. The hyperelastic material model very much replicated the vinyl material behavior well; therefore it is used to validate the head-form model.

MEASUREMENT OF FRICTION

The coefficient of friction between the steel plate and the head-form was measured to define the kinematic contact characteristics of the hyperelastic model with the plate. It adds external coulomb friction afforded by the plate to the simulation. Figure 7 shows the apparatus used to measure the coefficient of friction. The mass of the head-form is 4.5 kg, and the normal force in this test is 4.5 kg x 9.81 m/s^2 = 44.15 N. The friction force, F required to move the head-form on the steel plate was found experimentally to be between 17 N to 20 N. The coefficient of friction was calculated to be in the range of 0.38 to 0.44 using the equation

$$\mu = F/N \quad (3)$$

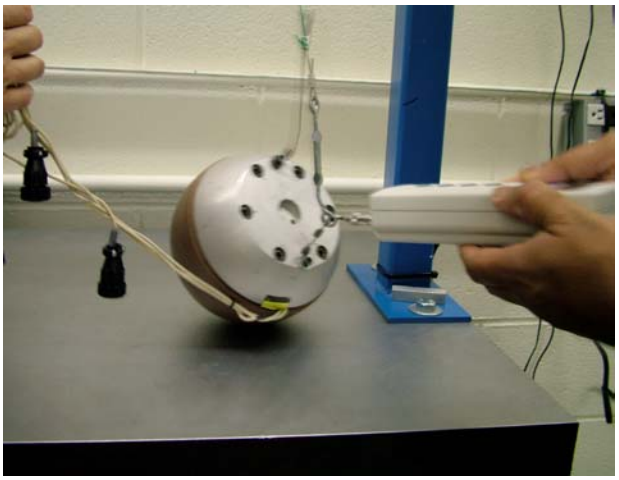

Figure 7 Measurement of friction between the vinyl skin and steel plate

VALIDATION OF THE IHRA HEAD-FORM MODEL

To verify that the hyperelastic material model for the vinyl adequately represented the IHRA adult head-form model's response, the IHRA adult head-form was dropped from four different drop heights of 356 mm, 500 mm, 880 mm and 950 mm and the results were compared with the corresponding MADYMO simulations.

IHRA child head-form model

The MADYMO model of the IHRA child head-form differs from the IHRA adult head-form only in mass, center of gravity and moment of inertia. Hence, these parameters are changed in the MADYMO head-form model to represent the child head-form. The MADYMO child head-form model was used to simulate the certification test to check whether the peak acceleration was within the range of 245 to 300 g (Table 1).

PARAMETER SENSITIVITY ANALYSIS

MADYMO simulations of IHRA adult and child head-form certification drop tests were conducted to study the sensitivity of head-form parameters to impact. While varying one parameter, the other parameters were fixed. For example when the mass was varied, the diameter was fixed as 165 mm and the center of gravity of the head-form and the location of the accelerometers were fixed at the center of the sphere. The mass was fixed at 4.5 kg for the adult head-form and 3.5 kg for the child head-form when the other parameters were varied. Tables 3 and 4 show the test matrix for the parameter sensitivity analysis of the IHRA adult and child head-forms respectively using MADYMO. With respect to the parameters, the adult and child head-forms are different only in mass and moment of inertia. The values and tolerances of the diameter, center of gravity and location of accelerometer are the same for both the head-forms. Tests number 1 – 5 in Tables 3 and 4 show the mass test matrix for the IHRA adult and child head-forms respectively. Tests number 6 – 10 in Tables 3 and 4 show the diameter test matrix for the IHRA adult and child head-forms respectively. Tests number 11 – 22 in Tables 3 and 4 show the test matrix for the location of the center of gravity with respect to the center of the sphere for the IHRA adult and child head-forms respectively. Tests number 23 – 34 in Tables 3 and 4 show the test matrix for location of the accelerometer with respect to the center of the sphere for the IHRA adult and child head-forms respectively.

RESULTS AND DISCUSSION

VALIDATION OF THE IHRA HEAD-FORM MODEL

The MADYMO simulation was implemented with the adjusted hyperelastic parameters A and B. It should be noted that hyperelasticity accounts for the stiffness characteristics of the vinyl but does not adequately represent the damping characteristics, although friction is added at the contact between the vinyl and the impact surface. Hence, without adding proper damping to the material model, the results were still not close to the laboratory drop results. Although the error in peak acceleration was less than –3%, HIC error was as high as 46%. To address this deficiency, various general damping coefficients were used to minimize the error between the simulation response and the laboratory test response. It was found that a value of 30,000 Ns/m for the damping coefficient produced a result that was comparable with the laboratory drop for the certification test as shown in Figure 8. This shows that the vinyl skin material is complex with properties of stiffness, hysteresis, relaxation, and damping which must be taken into consideration. In addition these properties are rate dependent.

Figure 8 shows the comparison of results obtained in a MADYMO simulation and a laboratory certification test for a drop height of 356 mm. The peak resultant acceleration obtained from the MADYMO simulation was 8% less than that obtained from the laboratory drop test. Table 5 compares the peak acceleration and HIC values obtained from the laboratory drop tests and MADYMO simulations for the four drop heights.

Table 3 Test matrix for the parameter sensitivity analysis of the IHRA adult head-form MADYMO model

Test No.	Mass (kg)	Diameter (mm)	Center of gravity location with respect to the center of the sphere (mm)			Accelerometer location with respect to the center of the sphere (mm)		
			X	Y	Z	X	Y	Z
1	4.4	165	0	0	0	0	0	0
2	4.45	165	0	0	0	0	0	0
3	4.5	165	0	0	0	0	0	0
4	4.55	165	0	0	0	0	0	0
5	4.6	165	0	0	0	0	0	0
6	4.5	164	0	0	0	0	0	0
7	4.5	164.5	0	0	0	0	0	0
8	4.5	165	0	0	0	0	0	0
9	4.5	165.5	0	0	0	0	0	0
10	4.5	166	0	0	0	0	0	0
11	4.5	165	0	0	5	0	0	0
12	4.5	165	0	0	10	0	0	0
13	4.5	165	0	0	-5	0	0	0
14	4.5	165	0	0	-10	0	0	0
15	4.5	165	0	5	0	0	0	0
16	4.5	165	0	10	0	0	0	0
17	4.5	165	0	-5	0	0	0	0
18	4.5	165	0	-10	0	0	0	0
19	4.5	165	5	0	0	0	0	0
20	4.5	165	10	0	0	0	0	0
21	4.5	165	-5	0	0	0	0	0
22	4.5	165	-10	0	0	0	0	0
23	4.5	165	4.3	-0.4	0.55	0	0	5
24	4.5	165	4.3	-0.4	0.55	0	0	10
25	4.5	165	4.3	-0.4	0.55	0	0	-5
26	4.5	165	4.3	-0.4	0.55	0	0	-10
27	4.5	165	4.3	-0.4	0.55	0	5	0
28	4.5	165	4.3	-0.4	0.55	0	10	0
29	4.5	165	4.3	-0.4	0.55	0	-5	0
30	4.5	165	4.3	-0.4	0.55	0	-10	0
31	4.5	165	4.3	-0.4	0.55	5	0	0
32	4.5	165	4.3	-0.4	0.55	10	0	0
33	4.5	165	4.3	-0.4	0.55	-5	0	0
34	4.5	165	4.3	-0.4	0.55	-10	0	0

In Table 5, the peak acceleration error is positive whereas the HIC error is negative for all four drop heights for the simulation compared with the laboratory tests. The MADYMO simulation HIC is greater than the laboratory drop HIC because of shorter duration of the acceleration pulse and a smaller difference in amplitude illustrated by the difference in the curve shapes. Had the actual values for the material parameters A and B been used in the simulation, it is expected that the response would match the laboratory drop test response more closely. During the laboratory drop test, the test set up (Figure 5) used for dropping the head-form that included the string support mechanism had a constraint that limited the maximum height of the head-form drop to 500 mm. In this test set up (Figure 5), the head-form is held at the desired height before the drop with the help of strings. The string is instantaneously detached from the top to initiate the drop. The string is used to precisely maintain the desired drop height and to avoid the rotation of the head-form, which might be caused while dropping the head-form by hand. For the 880 mm and 950 mm drop heights, this set up could not be used and the head-form was released by hand onto a steel plate placed on the ground.

Table 4 Test matrix for the parameter sensitivity analysis of the IHRA child head-form MADYMO model

Test No.	Mass (kg)	Diameter (mm)	Center of gravity location with respect to the center of the sphere (mm)			Accelerometer location with respect to the center of the sphere (mm)		
			X	Y	Z	X	Y	Z
1	3.4	165	0	0	0	0	0	0
2	3.45	165	0	0	0	0	0	0
3	3.5	165	0	0	0	0	0	0
4	3.55	165	0	0	0	0	0	0
5	3.6	165	0	0	0	0	0	0
6	3.5	164	0	0	0	0	0	0
7	3.5	164.5	0	0	0	0	0	0
8	3.5	165	0	0	0	0	0	0
9	3.5	165.5	0	0	0	0	0	0
10	3.5	166	0	0	0	0	0	0
11	3.5	165	0	0	5	0	0	0
12	3.5	165	0	0	10	0	0	0
13	3.5	165	0	0	-5	0	0	0
14	3.5	165	0	0	-10	0	0	0
15	3.5	165	0	5	0	0	0	0
16	3.5	165	0	10	0	0	0	0
17	3.5	165	0	-5	0	0	0	0
18	3.5	165	0	-10	0	0	0	0
19	3.5	165	5	0	0	0	0	0
20	3.5	165	10	0	0	0	0	0
21	3.5	165	-5	0	0	0	0	0
22	3.5	165	-10	0	0	0	0	0
23	3.5	165	3.3	0.5	-2.5	0	0	5
24	3.5	165	3.3	0.5	-2.5	0	0	10
25	3.5	165	3.3	0.5	-2.5	0	0	-5
26	3.5	165	3.3	0.5	-2.5	0	0	-10
27	3.5	165	3.3	0.5	-2.5	0	5	0
28	3.5	165	3.3	0.5	-2.5	0	10	0
29	3.5	165	3.3	0.5	-2.5	0	-5	0
30	3.5	165	3.3	0.5	-2.5	0	-10	0
31	3.5	165	3.3	0.5	-2.5	5	0	0
32	3.5	165	3.3	0.5	-2.5	10	0	0
33	3.5	165	3.3	0.5	-2.5	-5	0	0
34	3.5	165	3.3	0.5	-2.5	-10	0	0

Hence the prospect of maintaining the desired height accurately and avoiding rotation of the head-form during the drop became difficult. An error of approximately +/- 20 mm was possible in the measurement of the height for the 880 mm and 950 mm drops. From Table 5 it can be seen that the errors for peak acceleration and HIC for the four drops are within 10% except for the HIC error of the 880 mm drop. It is possible that the actual drop height was less than the desired 880 mm height. With a decreased drop height in the simulation, the peak acceleration and HIC would decrease accordingly, thereby decreasing the error in HIC value for this drop if the actual drop height was less than 880 mm. For instance, the error in HIC dropped to -15% and the peak acceleration error increased to only 3% while dropping the head-form from 860 mm instead of 880 mm in the MADYMO simulation.

The peak acceleration obtained in the certification test simulation of the IHRA child head-form is 270 g, which is well within the range of 245 to 300 g (Table 1).

Table 5 Comparison of MADYMO simulation results and laboratory drop results for the four drop heights

Drop height (mm)	Peak Acceleration (G)			HIC		
	MADYMO	Drop	% error	MADYMO	Drop	% error
376	234	255	8.2	913	875	-4.3
500	279	301	7.3	1372	1258	-9.1
880	399	405	1.5	3099	2595	-19.4
950	419	428	2.1	3467	3160	-9.7

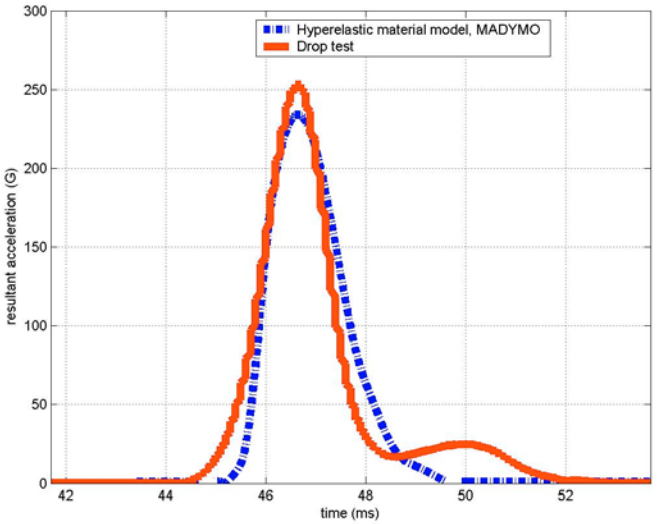

Figure 8 Comparison of MADYMO simulation results and laboratory drop results for a drop height of 376 m

Table 6 Results of varying the mass within the limits of mass tolerance in the IHRA head-forms using MADYMO

S.No.	Adult head-form			Child head-form		
	Mass (kg)	Peak acceleration (G)	HIC	Mass (kg)	Peak acceleration (G)	HIC
1	4.4	234.2	915	3.4	259.6	1039.8
2	4.45	233.3	909.9	3.45	258	1032.3
3	4.5	232.1	904.8	3.5	256.6	1025.1
4	4.55	231.1	899.8	3.55	255.1	1018
5	4.6	230.1	894.9	3.6	253.7	1011

Table 7 Results of varying the diameter within the limits of diameter tolerance in the IHRA head-forms using MADYMO

S.No.	Diameter (mm)	Adult head-form		Child head-form	
		Peak Acceleration (G)	HIC	Peak Acceleration (G)	HIC
1	164	239.5	949.5	264.9	1076.2
2	164.5	235.9	927.7	260.8	1051.2
3	165	232.1	904.8	256.6	1025.1
4	165.5	229.1	887.4	253.1	1005.2
5	166	225.9	869.1	249.5	984.1

PARAMETER SENSITIVITY ANALYSIS

The results of varying the mass within the limits of mass tolerance for both the adult and child head-forms are given in Table 6. With increase in mass, the peak acceleration and HIC values decrease. Assuming the head-form to be a simple spring mass system, the relationship between the contact force and displacement is given by,

$ma=k\Delta x$ (4)

where,

m – Mass of the head-form
a – acceleration of the head-form
K – Stiffness of the spring
Δx – deflection of the spring

With increase in mass, the acceleration will decrease if the contact force $k\Delta x$ is constant. This also explains why the peak acceleration range (Table 1) for the child head-form is greater than that of the adult head-form as both the head-forms have the same vinyl skin. The peak acceleration values for both the head-forms were well within the given acceleration range for the different masses within the limits of mass tolerance.

The results of varying the diameter within the limits of diameter tolerance for both the adult and child head-forms are given in Table 7. For varying the head-form diameter within the limits of diameter tolerance, the inner diameter of the vinyl skin is maintained as a constant and the outer diameter is changed which resulted in the thickness change of the vinyl skin. With an increase in the thickness of the vinyl skin, there is more room for deformation and hence the deceleration decreases as listed in Table 7. The peak acceleration values for both the head-forms are well within the acceleration range for the different diameters.

The results of varying the center of gravity within the limits of center of gravity tolerance for both the adult and child head-forms are given in Table 8. As the head-form is dropped along the Z–axis, changing the position of the center of gravity along this axis did not change the results as shown in Table 8. Both the head-form models were symmetrical about the Z–axis in MADYMO; hence, the result was the same in the positive and negative directions of the X and Y-axes. The results are well within the given acceleration range for both the head-forms while varying the location of center of gravity within the limits of center of gravity tolerance.

Table 8 Results of varying the location of the center of gravity within the limits of center of gravity tolerance in the IHRA head-forms using MADYMO

S.No.	Location of COG w.r.t center of sphere (mm)			Adult head-form		Child head-form	
	X	Y	Z	Peak acceleration (G)	HIC	Peak acceleration (G)	HIC
1	0	0	0	232.1	904.8	256.6	1025.1
2	0	0	5	232.1	904.8	256.6	1025.1
3	0	0	10	232.1	904.8	256.6	1025.1
4	0	0	-5	232.1	904.8	256.6	1025.1
5	0	0	-10	232.1	904.8	256.6	1025.1
6	0	5	0	232.7	906.4	257.2	1026.8
7	0	10	0	234.4	911.6	259	1032.4
8	0	-5	0	232.7	906.6	257.2	1027
9	0	-10	0	234.4	912	259.1	1032.8
10	5	0	0	232.7	906.5	257.2	1026.9
11	10	0	0	234.4	911.8	259.1	1032.6
12	-5	0	0	232.7	906.5	257.2	1026.9
13	-10	0	0	234.4	911.8	259.1	1032.5

Table 9 Results of varying the location of accelerometer within the limits of accelerometer location tolerance in the IHRA head-forms using MADYMO

S.No.	Location of accelerometer w.r.t center of sphere (mm)			Adult head-form		Child head-form	
	X	Y	Z	Peak acceleration (G)	HIC	Peak acceleration (G)	HIC
1	0	0	0	232.9	907.2	265.2	1077.2
2	0	0	5	232.9	907.4	265.2	1077.3
3	0	0	10	232.9	907.8	265.2	1077.5
4	0	0	-5	232.9	907.1	265.2	1077.1
5	0	0	-10	232.9	907.1	265.2	1077.1
6	0	5	0	234.2	919	265	1075.4
7	0	10	0	235.6	931	264.8	1073.7
8	0	-5	0	231.6	895.4	265.4	1079
9	0	-10	0	230.3	883.8	265.6	1080.8
10	5	0	0	231.5	894.5	263.9	1065.4
11	10	0	0	230	882	262.6	1053.7
12	-5	0	0	234.3	920	266.4	1089.1
13	-10	0	0	235.8	932.8	267.7	1101.1

The results of varying the seismic mass location within the limits of seismic mass location tolerance for both the adult and child head-forms are given in Table 9. In the case of varying the location of the accelerometer for both the head-forms, the center of gravity was maintained as the actual center of gravity. As the head-form is dropped along the Z-axis without any rotation, varying the accelerometer position while maintaining the center of gravity of the head-form at the center of the sphere did not change the results considerably. Using the actual center of gravity in the MADYMO model resulted in the rotation of the head-form during impact, thereby allowing the study of variation of the accelerometer position as shown in Table 9. Along the Z–axis, the results did not change because it is the axis along which the head-form is dropped. The results were well within the given acceleration range for both the head-forms.

Table 10 shows the summary of results of the parameter sensitivity analysis of both the adult and child head-forms. For the adult head-form, with 1 kg increase in mass, the peak acceleration decreased by less than 1% and the HIC decreased by less than 2%. For the child head-form, with 1 kg increase in mass, both the peak acceleration and HIC decreased by less than 2%. With 1 mm increase in diameter, the peak acceleration decreased by less than 4% and the HIC decreased by less than 5% for both the adult and child head-forms. Varying the center of gravity along the Z-axis neither changed the peak acceleration nor the HIC. Positioning the center of gravity within a distance of 10 mm from the center of the sphere in either X or Y-axes increased the peak acceleration and HIC by less than 1% for both the adult and child head-forms. Positioning the accelerometer within a distance of 10 mm from the center of the sphere changed the peak acceleration by less than 2% and HIC by less than 4% for both the adult and child head-forms.

In summary, a hyperelastic material model for the vinyl skin was found to best represent the response of the IHRA head-forms. The MADYMO model of the IHRA adult head-form was validated at several drop velocities to assess its versatility. Finally, the MADYMO head-form model was used to evaluate the effect of mass and geometric parameters on its response.

Table 10 Summary of results of variation of mass, diameter, center of gravity location and accelerometer seismic mass location.

		Adult head-form		Child head-form	
		Peak acceler-ation	HIC	Peak acceler-ation	HIC
Mass	For 0.1 kg increase	< 1%	< 2%	<2 %	<2 %
Diameter	For 1 mm increase	< 4%	< 5%	< 4%	<5 %
Center of gravity	For 10 mm in X	< 1%	< 1%	< 1%	< 1%
	For 10 mm in Y	< 1 %	< 1 %	< 1 %	< 1%
	For 10 mm in Z	0%	0%	0%	0%
Accelero-meter seismic mass location	For 10 mm in X	< 2%	< 4%	< 2%	< 4%
	For 10 mm in Y	< 2%	< 4%	< 2%	< 4%
	For 10 mm in Z	0%	0%	0%	0%

CONCLUSIONS

MADYMO models of the IHRA adult and child head-forms were developed. In the MADYMO model of the head-form, the aluminum core and the accelerometer mount were represented by a multibody sphere whereas the vinyl skin was modeled with finite elements using ABAQUS and imported into MADYMO. The most significant part in modeling the MADYMO head-form model was to determine a suitable material model for the vinyl skin. After examining the various material models, it was found that a hyperelastic material model is more appropriate to model this vinyl material. The MADYMO model of the IHRA adult head-form was validated with laboratory head-form drop tests of different drop heights. The MADYMO model closely replicated the laboratory drop test response with slight deviations, which can be attributed to the use of approximate values for the hyperelastic material parameters A and B. The peak acceleration was well within 9% error for the four different drop heights and the HIC error was within -10% for three out of the four drop heights.

Parameter sensitivity analysis was conducted by varying the head-form parameters within their respective limits of tolerances and it was found that the peak acceleration was well within the given range for both the adult and child head-forms. The change in the diameter within the tolerances produces considerable change in the peak acceleration and HIC values. There is no change in the results for varying the center of gravity or the accelerometer seismic mass location along the Z–axis within the given tolerance of 10 mm as this the direction along which the head-form is dropped.

ACKNOWLEDGMENTS

The work was supported by NHTSA. We appreciate all the help and input provided by the VRTC staff.

REFERENCES

1. Barbat, S. D. Jeong, H. Y. and Prasad, P. “Finite element modeling and development of the deformable featureless headform and its applications to vehicle interior head impact testing”, SAE paper number 960104, 1996

2. Bilkhu, S. S. Uduma, K. Fo. M. and Nu, G. S. “Development of a rubber-like headform skin model for predicting the head injury criterion (HIC)”, SAE paper number 950833, 1995

3. Chidester, C. Isenberg, R. “Final Report – The Pedestrian Crash Data Study”, U.S. Department of Transportation, National Highway Traffic Safety Administration

4. Chou, C. C. Barbat, S. D. Liu, N. Li, G. F. Wu, F. zhao, Y. “Additional notes on finite element models of deformable featureless head-form”, SAE paper number 970164, 1997

5. Deb, A. Ali, T. “A lumped parameter-based approach for simulation of automotive head-form impact with countermeasures”, International journal of Impact Engineering 30 (2004) 521-539

6. Harruff, R. C. Avery, A. Alter-Pandya, Amy S. “Analysis of Circumstances and Injuries in 217 Pedestrian Traffic Fatalities”, Accident Analysis & Prevention 30 (1998) pp. 11-20

7. “International Harmonized Research Activities Pedestrian Safety Working Group 2001 Report”, IHRA/PA/200

8. Kamalakkannan, S. Wiechel, J. Guenther, D. “Experimental determination of hyperelastic material parameters” Technical brief submitted to Journal of Biomechanics

9. Kleiven, S. Hardy, W. N. “Correlation of an FE Model of the Human Head with Local Brain Motion – Consequences for Injury Prediction”, STAPP Car Crash Journal (November 2002) 46:123-144

10. Konosu, A. Ishikawa, H. Kant, R. “Development of Computer Simulation Models for Pedestrian Subsystem Impact Tests”, JSAE 21 (2000) 109-115

11. Nakahama, R. Ikeno, H. Sakurai, T. Sato, Y. “A study on a simulation of a head-form impact against plastic plates”, SAE worldwide passenger car conference and exposition, SAE paper number 922085, 1992

12. Peng, R. Y. Bongard, F. S. “Pedestrian Versus Motor Vehicle Accidents: an Analysis of 5,000 Patients”, Journal of the American College of Surgeons 189 October 1999 pp. 343-348

13. Ruan, J. S. Khalil, T. B. King, A. I. “Finite Element Modeling of Direct Head Impact”, STAPP Car Crash Journal (1993) 37:69-81

14. Sugita, N. Yasuki, T. Nagamori, M. “A finite element analysis as optimization of energy absorbing structure in head impact”, Automotive body interior and safety systems, proceedings of the 1995 international body engineering conference, pp 55-62, Detroit 1995

15. Takhounts, E. G. Eppinger, R.H. “On the Development of the SIMon Finite Element Head Model”, STAPP Car Crash Journal, Vol. 47 (October 2003) pp. 107-133

16. TNO (2003): MADYMO Theory Manual, Version 6.1, TNO – Automotive, Delft, The Netherlands

17. Willinger, R. Kang, H. S. Baye, M. D. “Development and Validation of a Human Head Mechanical Model”, Comptes Rendus de lAcademie des Sciences Series IIB Mechanics Physics Astronomy (January 1999) 327:125-131

18. Zhang, L. Yang, K. H. Dwarampudi, R. Omori, K. Li, T. Chang, K. Hardy, W. N. Khalil, T. B. King, A. I. “Recent Advances in Brain Injury Research: A New Human Head Model Development and Validation”, STAPP Car Crash Journal (November 2001) 45:369-394

19. http://www.factbook.net/EGRF_Regional_analyses_Africa.htm

CONTACT

Sarath Babu Kamalakkannan, M.S
Mechanical Engineering
The Ohio State University
Email: Kamalakkannan.1@osu.edu
Phone: 614-598-0438